

Lattice techniques to investigate the strong CP problem: lessons from a toy model

David Albandeia,^{a,*} Guilherme Catumba^a and Alberto Ramos^a

^a*Instituto de Física Corpuscular (CSIC – University of Valencia), Parque Científico, C/Catedrático José Beltrán, 2, 46980, Paterna, Valencia, Spain*

E-mail: david.albandea@ific.uv.es

Recent studies have claimed that the strong CP problem does not occur in QCD, proposing a new order of limits in volume and topological sectors when studying observables on the lattice. We study the effect of the topological term on a simple quantum mechanical rotor that allows a lattice description. We particularly focus on recent proposals to face the challenging problems that this study poses in lattice QCD and that are also present in the quantum rotor, such as topology freezing and the sign problem.

The 41st International Symposium on Lattice Field Theory (LATTICE2024)
28 July - 3 August 2024
Liverpool, UK

*Speaker

1. Introduction

The QCD Lagrangian admits an additional renormalizable and gauge invariant term known as the θ term,

$$\delta\mathcal{L}_\theta = \theta q(x) \equiv \frac{\theta}{16\pi^2} \text{tr} F_{\mu\nu} \tilde{F}^{\mu\nu}, \quad (1)$$

where $\theta \in [0, 2\pi)$, is a free parameter of the model on which physical observables can potentially depend. This term would violate CP symmetry, but from experimental measurements of electric dipole moment of the neutron we know that θ must be extremely small, $|\theta| \lesssim 10^{-10}$ [1, 2]. The puzzle why it happens to be so small is known as the strong CP problem.

There have been many proposed solutions in the literature to explain the smallness of the θ angle, such as a Peccei-Quinn symmetry [3] and Nelson-barr type models [4, 5]. However, the strong CP problem is far from being settled, and there have been repeated debates about whether the θ angle affects physics at all, regardless of its value. Particularly, a recent proposal argues [6, 7] that expectation values in infinite volume can be obtained from expectation values at finite volume as

$$\langle O \rangle = \lim_{N \rightarrow \infty} \lim_{V \rightarrow \infty} \sum_{|Q| < N} \langle O \rangle_{Q,V} p_V(Q), \quad (2)$$

where O is an observable, $\langle \dots \rangle_{Q,V}$ denotes expectation value at fixed topological sector Q and finite volume V , $p_V(Q)$ is the distribution of topological charge at finite volume, and the volume is taken to infinity before the contributions from all topological sectors are summed. The consequence of such an order of limits, opposite to the conventional one, would be the absence of θ -dependence from observables, implying that there is no strong CP problem.

The θ -dependence is difficult to study in lattice QCD simulations because of several computational challenges, such as the sign problem [8, 9] and topology freezing [10–13]. However, the claims presented in Refs. [6, 7] should also hold in simpler models. The present work is based on Ref. [14] and is organized as follows: in Sec. 2, we study the order of limits of Eq. (2) in the one-dimensional quantum rotor, showing that it disagrees with the conventional one for the particular case of the topological susceptibility; in Secs. 3 and 4, we introduce two recently proposed algorithms to overcome both topology freezing and the sign problem, respectively; finally, in Sec. 5, we study the continuum limit of the topological susceptibility and the θ -dependence of the ground state of the spectrum of the quantum rotor with lattice simulations.

2. The quantum rotor

The quantum rotor is the simplest theory with topology and the presence of a θ term: it is a free particle of mass m on a ring, with Hamiltonian

$$H = -\frac{1}{2I} \left(\partial_\phi - \frac{\theta}{2\pi} \right)^2, \quad (3)$$

where ϕ is the angle representing the position of the particle in the ring (see Fig. 1 [left]), $I = mR^2$ is its moment of inertia, and $\theta \in [0, 2\pi)$ is a free parameter, analogous to the θ angle of QCD.

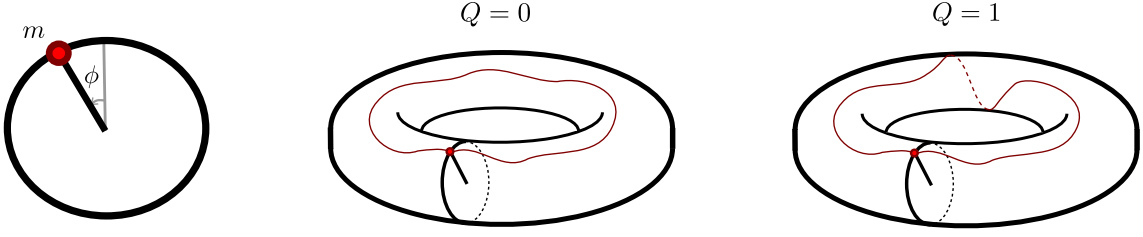


Figure 1: (Left) Representation of the quantum rotor. (Middle and right) Possible trajectories of the quantum rotor along a torus in the path integral representation, with topological charges $Q = 0$ and $Q = 1$.

The system can also be formulated as a path integral at finite temperature β and Euclidean volume $T = 1/\beta$ via the partition function [15, 16]

$$Z_T(\theta) = \int \mathcal{D}\phi e^{-S[\phi] + i\theta Q[\phi]}, \quad (4)$$

where action and topological charge in the continuum read

$$S[\phi] = \frac{I}{2} \int_0^T dt \dot{\phi}(t)^2, \quad Q[\phi] = \frac{1}{2\pi} \int_0^T dt \dot{\phi}(t) \in \mathbb{Z}, \quad (5)$$

where $-\pi < \phi(t) \leq \pi$ and periodic boundary conditions are imposed, i.e. $\phi(T) = \phi(0) + 2\pi n$ with $n \in \mathbb{Z}$. Additionally, topology can be easily visualized in this model, as the periodic boundary conditions make the trajectory of the particle live on the surface of a torus (see Fig. 1 [right]), where each trajectory can be classified with an integer Q : if the trajectory of a configuration does not wind around the torus, it has topological charge $Q = 0$; if it winds once around the torus, it has $Q = 1$.

This model can be trivially solved using the quantum mechanical formalism, and the energy levels of the system read

$$E_n = \frac{1}{2I} \left(n - \frac{\theta}{2\pi} \right)^2, \quad n \in \mathbb{Z}, \quad (6)$$

from which one can build the thermal partition function $Z_T(\theta) = \sum_{n \in \mathbb{Z}} e^{-TE_n} = \sum_{n \in \mathbb{Z}} e^{-\frac{T}{2I} (n - \frac{\theta}{2\pi})^2}$ and obtain the probability distribution of each topological sector,

$$p_T(Q) = \frac{1}{Z_T(\theta=0)} \frac{1}{2\pi} \int_{-\pi}^{\pi} d\theta Z_T(\theta) e^{-i\theta Q} = \frac{1}{Z_T(\theta=0)} \sqrt{\frac{2I\pi}{T}} \exp\left(-\frac{2I\pi^2}{T} Q^2\right). \quad (7)$$

With these results one can test the order of limits of Eq. (2). Particularly, the topological susceptibility in a finite volume V can be computed as

$$\chi_{t,V} = \frac{\langle Q^2 \rangle_V}{V}, \quad (8)$$

and studying the infinite volume limit as in Eq. (2) one finds

$$\chi_t = \lim_{N \rightarrow \infty} \lim_{T \rightarrow \infty} \frac{1}{T} \sum_{|Q| < N} Q^2 p(Q) = \lim_{N \rightarrow \infty} \lim_{T \rightarrow \infty} \frac{1}{T} \frac{\sum_{|Q| \leq N} Q^2 \exp(-\frac{2\pi^2 I}{T} Q^2)}{\sum_{|Q| \leq N} \exp(-\frac{2\pi^2 I}{T} Q^2)}, \quad (9)$$

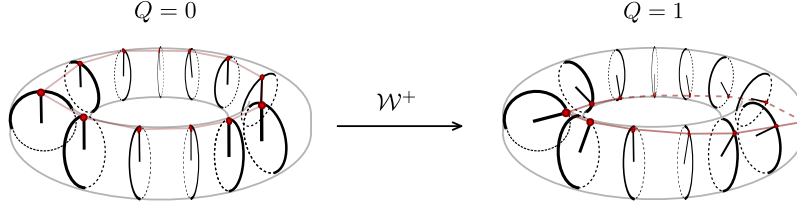


Figure 2: Winding transformation on a quantum rotor configuration on the lattice.

which is trivially zero. Alternatively, one can obtain the topological susceptibility in the zero temperature limit ($T \rightarrow \infty$) directly from the energy spectrum in Eq. (6), which reads

$$\chi_t \equiv \left. \frac{d^2 E_0(\theta)}{d\theta^2} \right|_{\theta=0} = \frac{1}{4\pi^2 I}. \quad (10)$$

This result can also be obtained with the conventional order of limits [14], and contradicts the result coming from the proposed order of limits in Eq. (9). In the following, we will validate the conventional order of limits using lattice simulations, for which we will need to deal with topology freezing and the sign problem.

3. Topology freezing and the winding HMC algorithm

Standard algorithms for lattice QCD, such as the Hybrid Monte Carlo (HMC) algorithm [17], are well-known to suffer from topology freezing: near the continuum limit, continuous update algorithms get trapped within a topological sector, thus failing to sample the full configuration space and leading to exponentially increasing autocorrelation times as the continuum limit is approached in a finite volume.

The topology freezing problem is also present in simple models such as the quantum rotor, making them useful testbeds for new algorithms aiming to tackle this problem. The spacetime discretization of the quantum rotor consists of $\hat{T} = T/a$ angle variables ϕ_t for $t \in \{0, \dots, \hat{T} - 1\}$ separated by a lattice spacing a . Here we will work with the so-called standard discretization of the action and topological charge,

$$S_{\text{st}}[\phi] = \frac{\hat{I}}{2} \sum_{t=0}^{\hat{T}-1} (1 - \cos(\phi_{t+1} - \phi_t)), \quad Q_{\text{st}}[\phi] = \frac{1}{2\pi} \sum_{t=0}^{\hat{T}-1} \sin(\phi_{t+1} - \phi_t), \quad (11)$$

where $\hat{I} = I/a$, as well as with the classical perfect discretization,¹

$$S_{\text{cp}}[\phi] = \frac{\hat{I}}{2} \sum_{t=0}^{\hat{T}-1} ((\phi_{t+1} - \phi_t) \bmod 2\pi)^2, \quad Q_{\text{cp}}[\phi] = \frac{1}{2\pi} \sum_{t=0}^{\hat{T}-1} ((\phi_{t+1} - \phi_t) \bmod 2\pi) \in \mathbb{Z}. \quad (12)$$

Note that both discretizations lead to the same continuum limit of Eq. (5) when taking $a \rightarrow 0$ along a line of constant physics with $T/I = \hat{T}/\hat{I} = \text{constant}$.

¹Note that the classical perfect topological charge, Q_{cp} , has a geometrical definition and is exactly an integer.

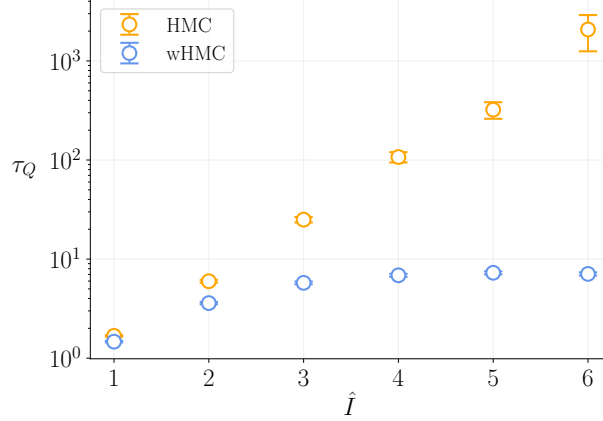


Figure 3: Autocorrelation time of Q as a function of \hat{I} for wHMC (blue) and HMC (orange), keeping $\hat{T}/\hat{I} = 100$, with the standard discretization of the action.

The simplest idea to build an algorithm that can sample topology efficiently is to find transformations between topological sectors. Such a topology-changing transformation can be easily built for the quantum rotor, for which we define the winding transformation by

$$\mathcal{W}^\pm : \phi_t \rightarrow \phi_t^{\mathcal{W}^\pm} = \phi_t \pm 2\pi t / \hat{T}, \quad \mathcal{W}^+ \mathcal{W}^- = I, \quad (13)$$

where the + (winding) or - (antiwinding) is common to all $t \in [0, \hat{T} - 1]$. As shown in Fig. 2, the transformation gradually winds the trajectory of a configuration around itself exactly once, such that $Q_{\text{cp}}(\phi^{\mathcal{W}^\pm}) = Q_{\text{cp}}(\phi) \pm 1$. This transformation can be easily embedded into a Metropolis algorithm with acceptance

$$p_{\text{acc}}(\phi^{\mathcal{W}^\pm} | \phi) = \min \left\{ 1, e^{-S[\phi^{\mathcal{W}^\pm}] + S[\phi]} \right\}, \quad (14)$$

and we denote the combination of this Metropolis step with the HMC algorithm as the winding HMC (wHMC) algorithm [18], which reestablishes ergodicity within the full configuration space if the acceptance is significant.

In Fig. 3 we show the scaling of autocorrelation times of the topological charge, τ_Q , from simulations with the HMC and wHMC algorithms. While the autocorrelations of HMC scale exponentially, as expected, the ones of wHMC eventually saturate, thus solving the topology freezing problem in this model.

4. The sign problem and truncated polynomials

The sign problem is caused by the imaginary term in Eq. (4), which for $\theta \neq 0$ is highly oscillatory and leads to uncertainties which grow exponentially with the volume of the system. A conventional workaround is to define $\theta_I \equiv i\theta \in \mathbb{R}$ so that the integrand becomes real and the system can be simulated using standard sampling algorithms. By performing simulations at different imaginary values of θ , one can then use the analyticity of an observable,

$$O(\theta) = O^{(0)} + O^{(1)}\theta + O^{(2)}\theta^2 + O(\theta^3), \quad O^{(n)} = \frac{1}{n!} \frac{\partial^n O}{\partial \theta^n} \Big|_{\theta=0}, \quad (15)$$

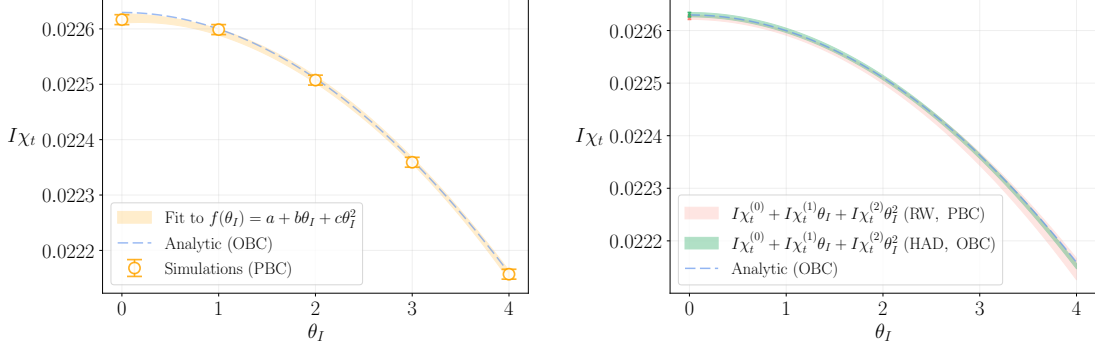


Figure 4: The θ_I dependence of $I\chi_t$ at $\hat{I} = 5$ and $\hat{T} = 100$ computed with different methods for periodic boundary conditions and the standard definitions of the action and topological charge. (Left): results (orange circles) from five different simulations with 100k uncorrelated configurations each, along with their fit to the functional form $f(\theta_I) = a + b\theta_I + c\theta_I^2$. (Right): results from single simulations with 500k uncorrelated configurations using reweighting and HAD (red and green points) at $\theta_I = 0$, along with the curve $I\chi_t^{(0)} + I\chi_t^{(1)}\theta_I + I\chi_t^{(2)}\theta_I^2$ (light-red and thick-green bands) obtained from the use of truncated polynomials. The reweighting was performed on a simulation with periodic boundary condition, while HAD was used with open boundary conditions. In both panels the analytic result from open boundary conditions is displayed (dashed line).

along with analytic continuation to obtain the expansion coefficients by performing fits to data. This is depicted in Fig. 4 (left), we show results of $I\chi_t$ for different values of θ_I .

An alternative method that allows to obtain arbitrarily high derivatives of θ just from a single simulation at $\theta = 0$ relies on the fact that a differentiable function f can be Taylor expanded around $x^{(0)}$. The construction of such Taylor expansion can be automatized for any arbitrarily complex function f by using the algebra of truncated polynomials [19]: if $\tilde{x} = x^{(0)} + x^{(1)}\epsilon + x^{(2)}\epsilon^2 + \dots + x^{(K)}\epsilon^K$ is a truncated polynomial of order K and we code all elementary mathematical functions of these polynomials, $f(\tilde{x})$ will be a truncated polynomial containing the first K derivatives of f . Truncated polynomials are a particular automatic differentiation technique and for our computations we use `FormalSeries.jl` [20], which can be used for any arbitrarily complicated function f , such as a computer program implementing reweighting or the HMC algorithm.

A particularly simple application of truncated polynomials to extract higher order derivatives from an existing simulation at $\theta = 0$ is by reweighting to $\theta \neq 0$ via the identity

$$\langle O(\phi) \rangle_\theta = \frac{\langle e^{i\theta Q} O(\phi) \rangle_{\theta=0}}{\langle e^{i\theta Q} \rangle_{\theta=0}}. \quad (16)$$

By replacing θ with the truncated polynomial $\tilde{\theta} = \sum_{k=0}^K \tilde{\theta}^{(k)} \theta^k$ with $\tilde{\theta}^{(1)} = 1$ and $\tilde{\theta}^{(k \neq 1)} = 0$, one automatically obtains the full analytical dependence of the Taylor expansion of $\langle O(\phi) \rangle_\theta$ with respect to θ up to order K from a single ensemble. This is shown in Fig. 4 (right), where by reweighting a single standard simulation at $\theta_I = 0$ with periodic boundary conditions we automatically obtain $I\chi_t^{(k)}$; particularly, we see that $I\chi_t^{(0)} + I\chi_t^{(1)}\theta_I + I\chi_t^{(2)}\theta_I^2$ agrees with the analytical result obtained with open boundary conditions.

Method	$\chi_t^{(0)} \times 10^{-3}$	$\chi_t^{(2)} \times 10^{-6}$
Fit	4.5238(16)	-6.08(48)
Reweighting	4.52501(76)	-5.99(25)
HAD	4.52604(83)	-5.980(34)

Table 1: Comparison of errors between different methods to obtain the θ_I -dependence, namely, the quadratic fit to the results from direct simulations at θ_I (Fig. 4 left), reweighting, and HAD (Fig. 4 right). These results correspond to simulations with $\hat{I} = 5$ and $\hat{T} = 100$, using the standard definitions of the action and topological charge.

However, a drawback of reweighting is that the denominator in Eq. (16) has disconnected contributions that are exponentially noisier with the size of the system. To solve this, one can apply the truncated polynomials directly into the HMC algorithm. Using the standard discretization of the model, the HMC equations of motion read

$$\begin{aligned} \dot{\phi}_t &= \frac{\partial H[\pi, \phi]}{\partial \pi_t} = \pi_t, \\ \dot{\pi}_t &= -\frac{\partial H[\pi, \phi]}{\partial \phi_t} = -I [\sin(\phi_t - \phi_{t-1}) - \sin(\phi_{t+1} - \phi_t)] + \frac{\theta_I}{2\pi} [\cos(\phi_t - \phi_{t-1}) - \cos(\phi_{t+1} - \phi_t)], \end{aligned} \quad (17)$$

where $H[\pi, \phi] = \sum_{t=0}^{\hat{T}-1} \pi_t^2/2 + S_{\text{st}}[\phi] - \theta_I Q_{\text{st}}[\phi]$ is the Hamiltonian of the system. By replacing θ_I by a truncated polynomial, $\tilde{\theta}_I$, we obtain a Markov chain of N samples, $\{\tilde{\phi}_{(i)}\}_{i=1}^N$, that carry the derivatives with respect to θ_I , and we denote this algorithm as Hamiltonian Automatic Differentiation (HAD). The Taylor expansion of observables is obtained by the computation of conventional expectation values using the samples $\{\tilde{\phi}_{(i)}\}_{i=1}^N$, and does not contain the noisy disconnected contributions of the reweighting technique.² In Fig. 4 (right), we show the curve $I\chi_t^{(0)} + I\chi_t^{(1)}\theta_I + I\chi_t^{(2)}\theta_I^2$ obtained from a single HAD simulation, and one can appreciate that the predictions for high θ_I are more accurate than the ones obtained by reweighting. The comparison can be seen more transparently in Tab. 1, where the error of the HAD algorithm is reduced by an order of magnitude with respect to the other methods at equivalent statistics.

5. Results

Fig. 5 (left) shows our results of a local version of the topological susceptibility, $\chi_t = \langle (\phi_1 - \phi_0)^2 \rangle$ —with which the choice of boundary conditions and the quantization of the topological charge is irrelevant—from simulations with periodic boundary conditions with both the standard and classical perfect discretizations at different values of the lattice spacing. The wHMC algorithm allowed us to perform simulations very close to the continuum, and our results agree with the analytical results obtained with open boundary conditions. All choices of boundary conditions and discretization lead to the continuum result in Eq. (10), validating the conventional order of limits.

Finally, in Fig. 5 we show our results of the linear θ -dependence of the ground state of the spectrum for different values of the lattice spacing, which from Eq. (6) reads $\Delta E_1 \equiv E_1 - E_0 =$

²However, the Metropolis accept-reject step is not differentiable and cannot be used with this method, so one must integrate the equations of motion with high enough precision to avoid systematic effects.

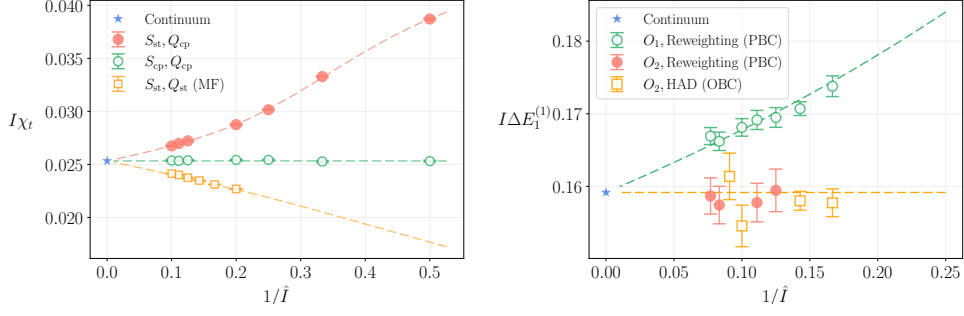


Figure 5: (Left) Continuum extrapolation of χ_t computed from $\langle(\phi_1 - \phi_0)^2\rangle$ at various $\{\hat{T}, \hat{I}\}$ at constant $T/I = 20$ with the standard action and classical topological charge (red, filled circles), with the classical action and topological charge (green, open circles) and from master field simulations with the standard action and topological charge (orange, open squares), all with periodic boundary conditions. The dashed lines represent the corresponding analytical results with open boundary conditions. (Right) Linear θ -correction to the first energy level, ΔE_1 , for a periodic lattice with the standard discretization of the action at different values of \hat{I} with constant $T/I = 20$. The results were obtained using the interpolating operator $O_1(t) = \phi_t$ with reweighting on a simulation with periodic boundary conditions (green, open circles), and using $O_2(t) = \sin(\phi_t)$ with HAD (yellow, open squares) and reweighting (red, filled circles) with open and periodic boundary conditions, respectively.

$\frac{1}{2I} \left(1 - \frac{\theta}{\pi}\right)$, obtained through the usual spectral decomposition of an interpolator with the same symmetries as the ground state. We use both reweighting and the HAD algorithm, for different choices of boundary conditions and interpolating operators, and conclude that the continuum limit agrees with the results from quantum mechanics—and disagree with the claims of Refs. [6, 7].

6. Conclusions

We have studied a recently proposed order of limits to study infinite-volume quantities which makes θ disappear from all physical observables of the theory. We have studied the continuum limit of the topological susceptibility and the first θ -dependence correction to the ground energy state of the quantum rotor, validating the conventional wisdom on the strong CP problem. Even though the system suffers from topology freezing and the sign problem, these were successfully overcome by the use of the wHMC algorithm and truncated polynomials. The generalization of these proposed algorithms to more complicated models is work in progress.

Acknowledgements

We acknowledge support from the Generalitat Valenciana Grant No. PROMETEO/2019/083, the European Projects No. H2020-MSCA-ITN-2019//860881-HIDDeN and No. 101086085-ASYMMETRY, and the National Project No. PID2020-113644GB-I00, as well as the technical support provided by the Instituto de Física Corpuscular, IFIC (CSIC-UV). D.A. acknowledges support from the Generalitat Valenciana Grants No. ACIF/2020/011 and No. PROMETEO/2021/083. G.C. and A.R. acknowledge financial support from the Generalitat Valenciana Grant No. CIDE-GENT/2019/040.

References

- [1] C. Abel et al., *Measurement of the Permanent Electric Dipole Moment of the Neutron*, *Phys. Rev. Lett.* **124** (2020) 081803 [2001.11966].
- [2] T. Chupp, P. Fierlinger, M. Ramsey-Musolf and J. Singh, *Electric dipole moments of atoms, molecules, nuclei, and particles*, *Rev. Mod. Phys.* **91** (2019) 015001 [1710.02504].
- [3] R.D. Peccei and H.R. Quinn, *Constraints imposed by CP conservation in the presence of pseudoparticles*, *Phys. Rev. D* **16** (1977) 1791.
- [4] A.E. Nelson, *Naturally Weak CP Violation*, *Phys. Lett. B* **136** (1984) 387.
- [5] S.M. Barr, *Solving the strong CP problem without the Peccei-Quinn symmetry*, *Phys. Rev. Lett.* **53** (1984) 329.
- [6] W.-Y. Ai, J.S. Cruz, B. Garbrecht and C. Tamarit, *Absence of CP violation in the strong interactions*, 2001.07152 .
- [7] W.-Y. Ai, J.S. Cruz, B. Garbrecht and C. Tamarit, *Consequences of the order of the limit of infinite spacetime volume and the sum over topological sectors for CP violation in the strong interactions*, *Phys. Lett. B* **822** (2021) 136616.
- [8] P. de Forcrand, *Simulating QCD at finite density*, *PoS LAT2009* (2009) 010 [1005.0539].
- [9] C. Gattringer and K. Langfeld, *Approaches to the sign problem in lattice field theory*, *Int. J. Mod. Phys. A* **31** (2016) 1643007 [1603.09517].
- [10] B. Alles, G. Boyd, M. D’Elia, A. Di Giacomo and E. Vicari, *Hybrid Monte Carlo and topological modes of full QCD*, *Phys. Lett. B* **389** (1996) 107 [hep-lat/9607049].
- [11] L. Del Debbio, H. Panagopoulos and E. Vicari, *Theta dependence of SU(N) gauge theories*, *JHEP* **08** (2002) 044 [hep-th/0204125].
- [12] L. Del Debbio, G.M. Manca and E. Vicari, *Critical slowing down of topological modes*, *Phys. Lett. B* **594** (2004) 315 [hep-lat/0403001].
- [13] ALPHA collaboration, *Critical slowing down and error analysis in lattice QCD simulations*, *Nucl. Phys. B* **845** (2011) 93 [1009.5228].
- [14] D. Albandea, G. Catumba and A. Ramos, *Strong CP problem in the quantum rotor*, *Phys. Rev. D* **110** (2024) 094512 [2402.17518].
- [15] N. Fjeldso, J. Midtdal and F. Ravndal, *Random walks of a quantum particle on a circle*, unpublished (1987) .
- [16] W. Bietenholz, R. Brower, S. Chandrasekharan and U.J. Wiese, *Perfect lattice topology: The Quantum rotor as a test case*, *Phys. Lett. B* **407** (1997) 283 [hep-lat/9704015].

- [17] S. Duane, A.D. Kennedy, B.J. Pendleton and D. Roweth, *Hybrid Monte Carlo*, *Phys. Lett. B* **195** (1987) 216.
- [18] D. Albandea, P. Hernández, A. Ramos and F. Romero-López, *Topological sampling through windings*, *Eur. Phys. J. C* **81** (2021) 873 [2106.14234].
- [19] A. Haro, *Automatic differentiation tools in computational dynamical systems*, unpublished (2011) .
- [20] A. Ramos, *FormalSeries.jl*, May, 2023. [10.5281/zenodo.7970278](https://doi.org/10.5281/zenodo.7970278).